

Godunov-type transport scheme in ICON

Implementation and results of idealised test cases

Daniel Reinert
Deutscher Wetterdienst

SRNWP-Workshop, 26.10.2009 Bad Orb

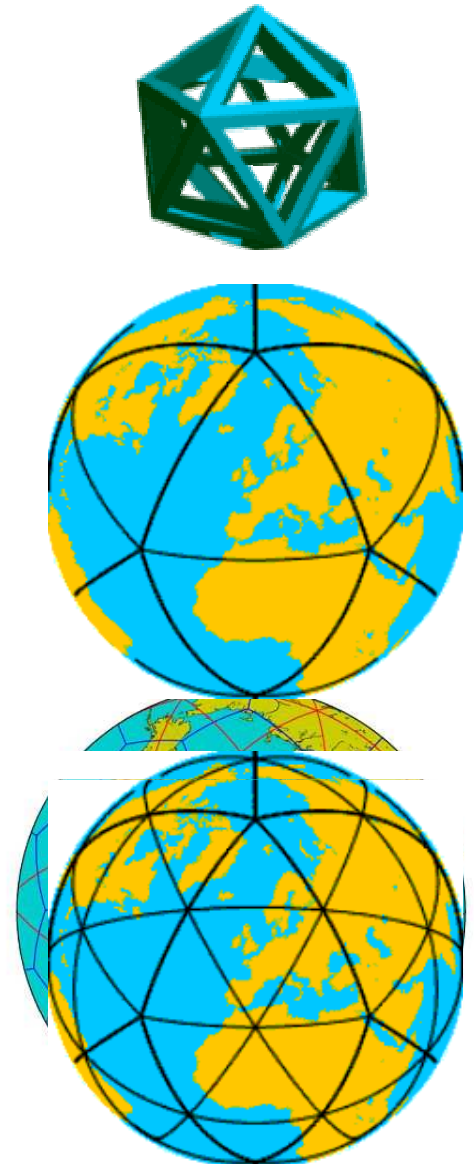
Outline

- I. The ICON-grid
- II. Transport on unstructured grids
 - Introduction into combined semi-Lagrangian finite-Volume thinking
- III. Currently implemented transport scheme
 - Reconstruction
 - Flux integration
- IV. Results of idealised test cases on the sphere
 - Solid body rotation
 - Deformational flow (static vortex)
- V. Summary and outlook

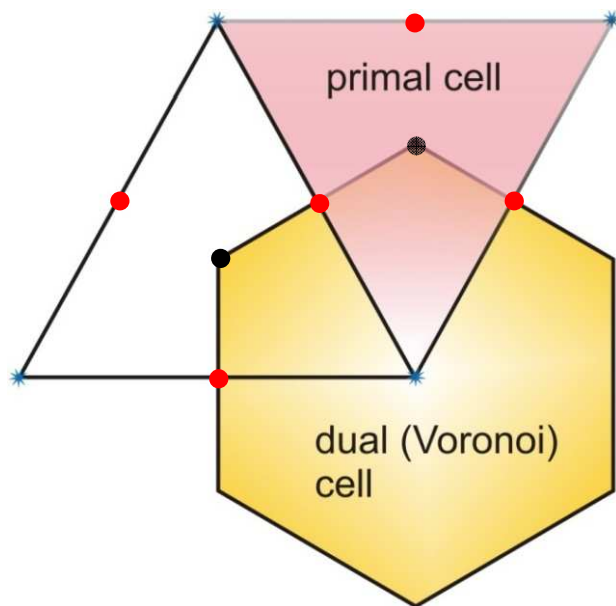
I. The ICON-grid

Grid topology and geometry

- Inscribe icosahedron inside the unit sphere
- The 12 vertices touching the surface define the basic mesh consisting of 20 spherical triangles.
- Further mesh refinement by one „root division“ followed by successive bisections (connect midpoints of the edges for each triangle by great circle arcs)
- Primal (Delaunay) grid: **triangles**
- Dual (Voronoi) grid: **hexagons**
(+ 12 pentagons at the icosahedron vertices)



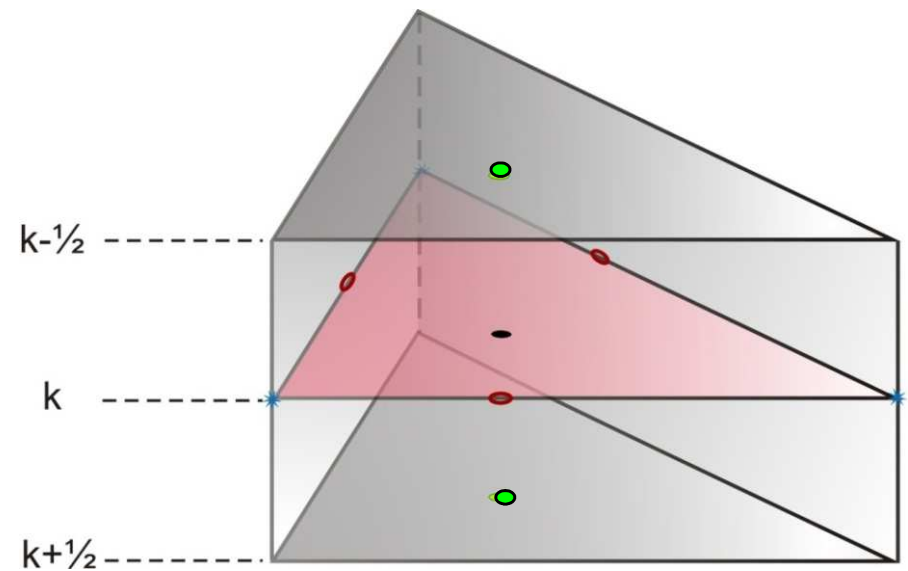
3D arrangement of the discrete variables



horizontal

C-type staggering

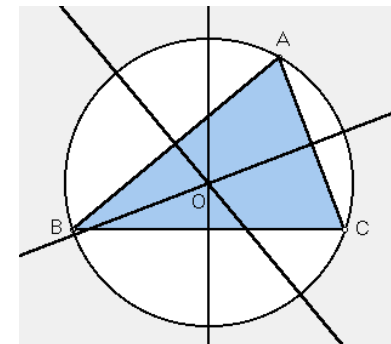
- T, q, p, Φ
- v_n
- * $\vec{k} \cdot (\vec{\nabla} \times \vec{v})$
- $\dot{\eta} \frac{\partial p}{\partial \eta}, \Phi, p$



vertical

➤ **Cell center:** center of triangle circumcircle

⇒ Arc connecting two mass points is orthogonal to and bisects triangle edge



II. Introduction into combined semi-Lagrangian finite-volume thinking

Problem formulation (horizontal)

- Find solution to

$$\frac{\partial \Psi}{\partial t} + \nabla \cdot (\vec{v} \Psi) = 0$$

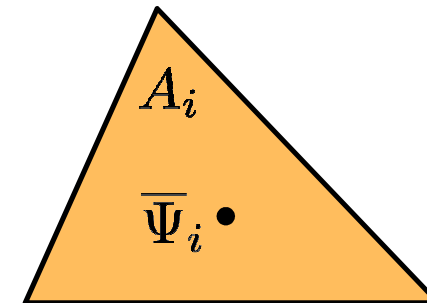
$$\begin{aligned} \Psi &= \rho q && \text{, if non-hydrostatic} \\ \Psi &= \Delta p q && \text{, if hydrostatic} \end{aligned}$$

on the sphere, using finite-Volume technique.

- Define control volume

- Discrete value at mass point is defined to be the average of the subgrid dist. over the control volume

$$\bar{\Psi}_i^n = \frac{1}{A_i} \iint_{A_i} \Psi(x, y, t_0) dA$$



A_i : control volume area

- Given $\bar{\Psi}_i$ at time t_0 we seek for a new set of $\bar{\Psi}_i$ at time $t_1 = t_0 + \Delta t$ as an approximate solution after a short time of transport.

Problem formulation

- Formally, the solution can be derived by integrating the continuity equation over the time interval $[t_0, t_1]$ and the control volume A_i

$$\int_{t_0}^{t_1} \iint_{A_i} \frac{\partial \Psi}{\partial t} dA dt = - \int_{t_0}^{t_1} \iint_{A_i} \vec{\nabla} \cdot (\vec{v} \Psi) dA dt$$

using Gauss-
theorem

$$\bar{\Psi}_i^{n+1} - \bar{\Psi}_i^n = - \frac{1}{A_i} \int_{t_0}^{t_1} \oint_{\partial A_i} (\Psi \vec{v} \cdot \vec{n}_i) dl dt$$

Assume triangular control volume and $\vec{v} = \text{const}$ for $t \in [t_0, t_1]$

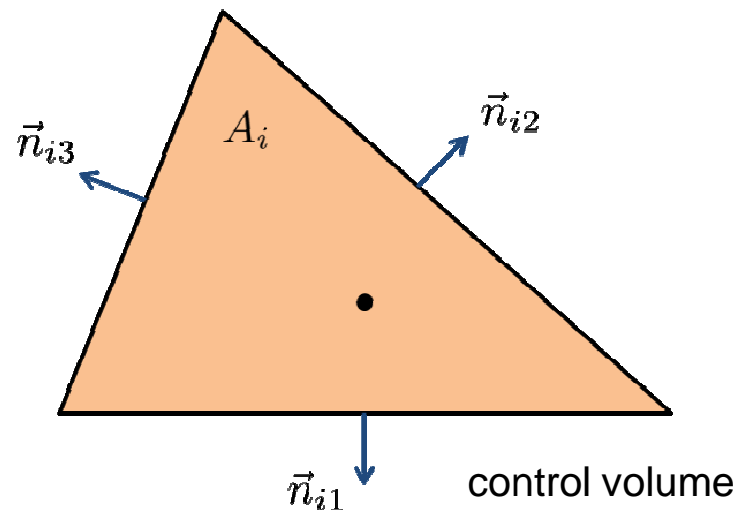
$$\bar{\Psi}_i^{n+1} = \bar{\Psi}_i^n - \frac{1}{A_i} \sum_{k=1}^3 \vec{F}_{ik} \cdot \vec{n}_{ik} \quad , \text{ with } \vec{F}_{ik} = \left(\iint_{A_{ik}} \Psi dA \right) \cdot \vec{n}_{ik}$$

- No approximation as long as we know the subgrid distribution Ψ and A_{ik} analytically; except for assumption of $\vec{v} = \text{const}$ for $t \in [t_0, t_1]$

What does it mean graphically ?

$$\bar{\Psi}_i^{n+1} = \bar{\Psi}_i^n - \frac{1}{A_i} \sum_{k=1}^3 \vec{F}_{ik} \cdot \vec{n}_{ik} \quad , \text{ with } \vec{F}_{ik} = \left(\iint_{A_{ik}} \Psi \, dA \right) \cdot \vec{n}_{ik}$$

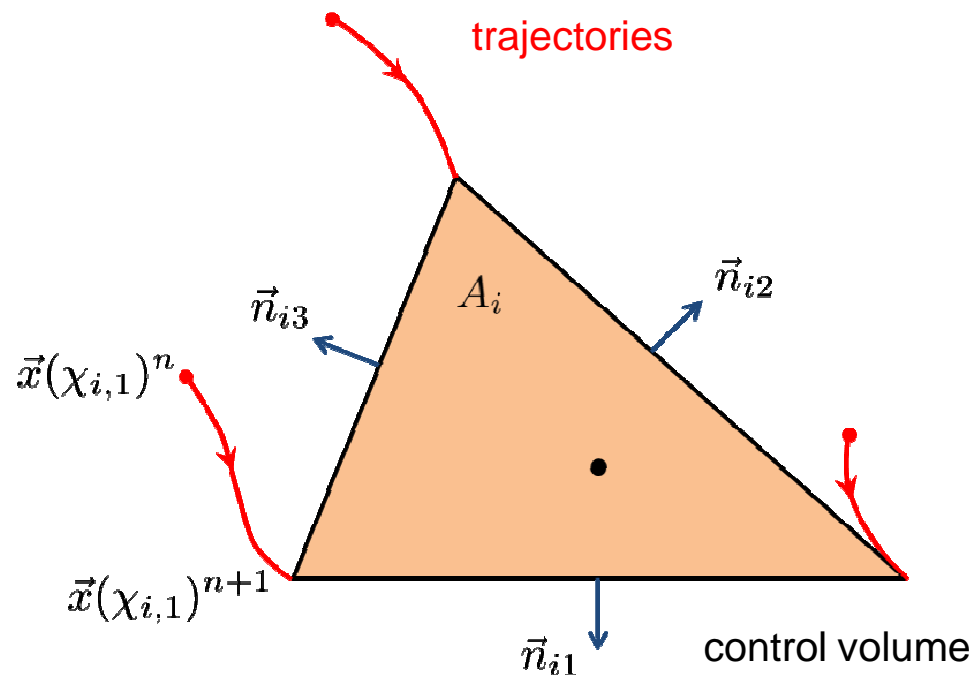
$\vec{n}_{ik}, \vec{\tilde{n}}_{ik}$: Unit normal pointing outward of A_i and A_{ik} , respectively



What does it mean graphically ?

$$\bar{\Psi}_i^{n+1} = \bar{\Psi}_i^n - \frac{1}{A_i} \sum_{k=1}^3 \vec{F}_{ik} \cdot \vec{n}_{ik} \quad , \text{ with } \vec{F}_{ik} = \left(\iint_{A_{ik}} \Psi \, dA \right) \cdot \vec{\hat{n}}_{ik}$$

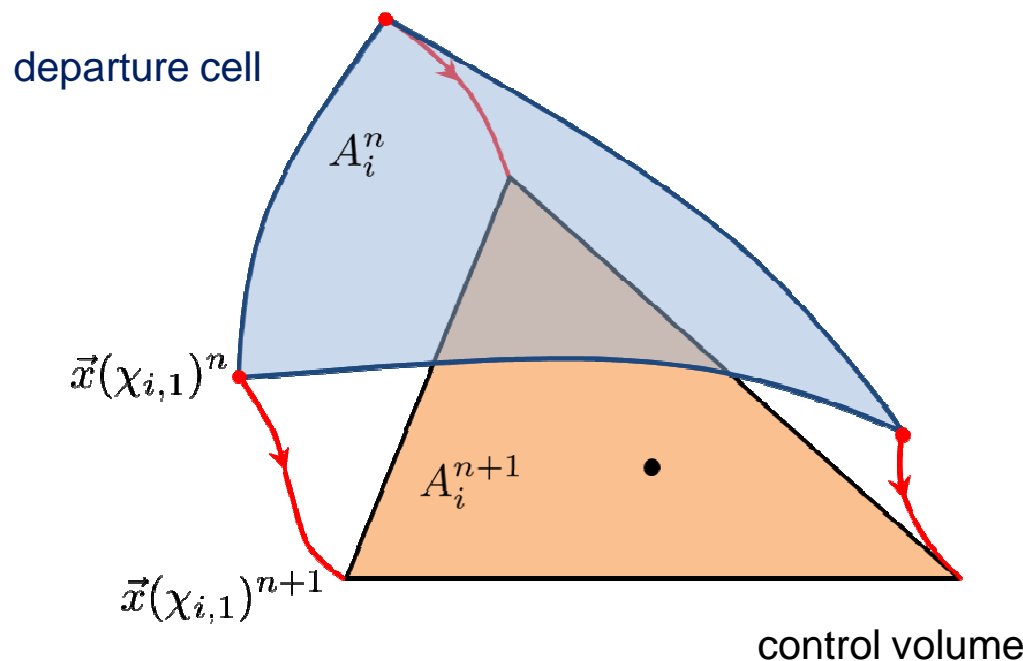
$\vec{n}_{ik}, \vec{\hat{n}}_{ik}$: Unit normal pointing outward of A_i and A_{ik} , respectively



What does it mean graphically ?

$$\bar{\Psi}_i^{n+1} = \bar{\Psi}_i^n - \frac{1}{A_i} \sum_{k=1}^3 \vec{F}_{ik} \cdot \vec{n}_{ik} \quad , \text{ with } \vec{F}_{ik} = \left(\iint_{A_{ik}} \Psi \, dA \right) \cdot \vec{\hat{n}}_{ik}$$

$\vec{n}_{ik}, \vec{\hat{n}}_{ik}$: Unit normal pointing outward of A_i and A_{ik} , respectively



semi-Lagrangian:

$$A_i^n \bar{\Psi}_{A_i^n} = A_i^{n+1} \bar{\Psi}_i^{n+1}$$



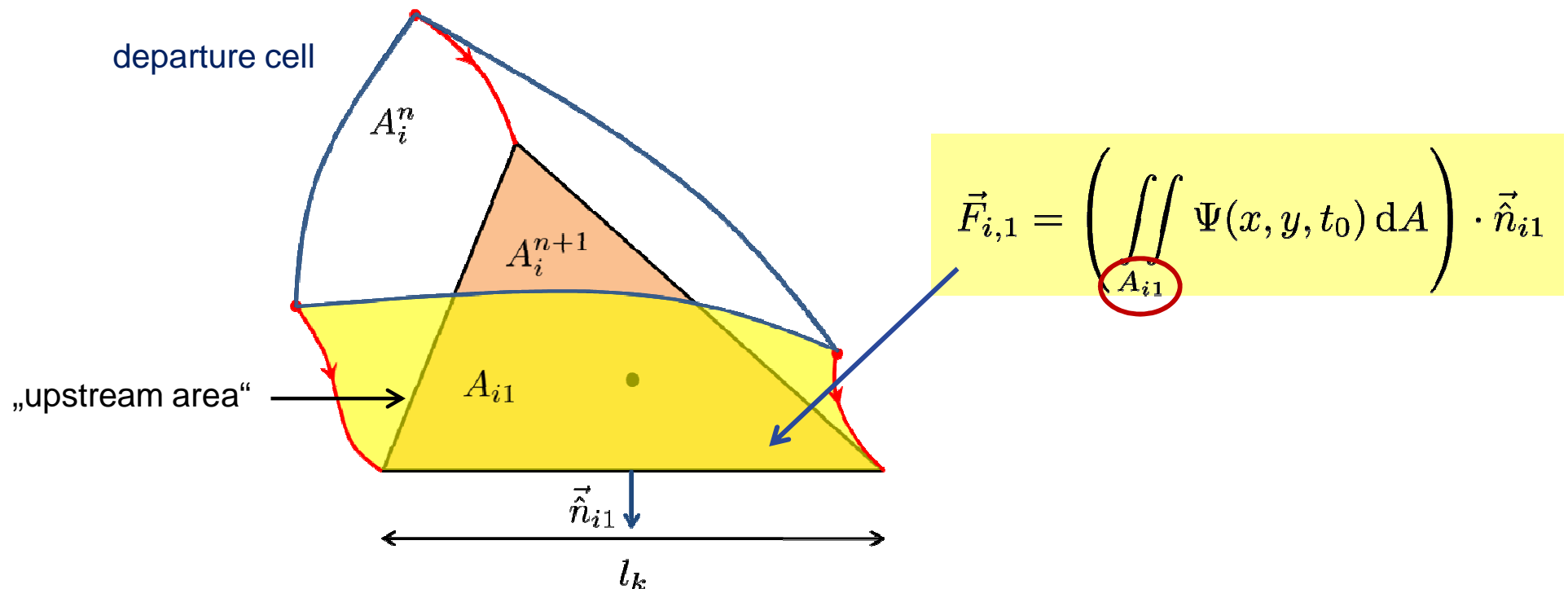
issue is down to calculating

$$\iint_{A_i^n} \Psi(x, y, t_0) \, dA$$

What does it mean graphically ?

$$\bar{\Psi}_i^{n+1} = \bar{\Psi}_i^n - \frac{1}{A_i} \sum_{k=1}^3 \vec{F}_{ik} \cdot \vec{n}_{ik} \quad , \text{ with } \vec{F}_{ik} = \left(\iint_{A_{ik}} \Psi \, dA \right) \cdot \vec{n}_{ik}$$

$\vec{n}_{ik}, \vec{\tilde{n}}_{ik}$: Unit normal pointing outward of A_i and A_{ik} , respectively



Algorithm

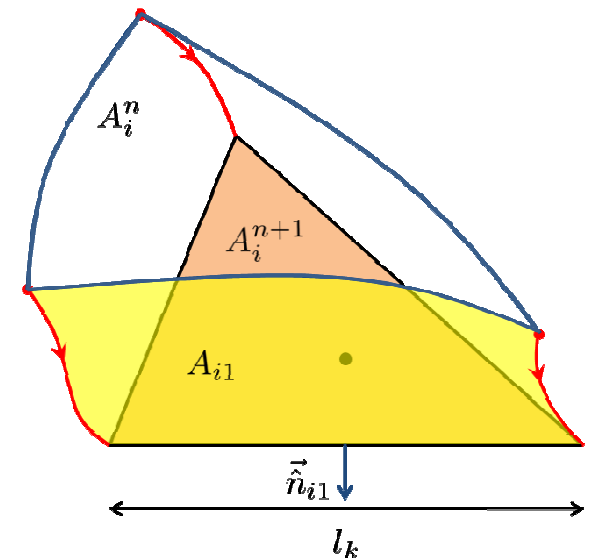
The numerical algorithm consists of three major steps

1. Determine the upstream area A_{ik} for the k^{th} edge
2. Determine the subgrid distribution $\Psi(x, y, t_0)$ for control volume i with cell average $\bar{\Psi}_i^n$
3. Integrate the subgrid distribution $\Psi(x, y, t_0)$ over the area A_{ik} .

$$\iint_{A_{ik}} \Psi(x, y, t_0) dA$$

plug in

$$\bar{\Psi}_i^{n+1} = \bar{\Psi}_i^n - \frac{1}{A_i} \sum_{k=1}^3 \vec{F}_{ik} \cdot \vec{n}_{ik} \quad , \text{ with } \vec{F}_{ik} = \left(\iint_{A_{ik}} \Psi dA \right) \cdot \vec{n}_{ik}$$

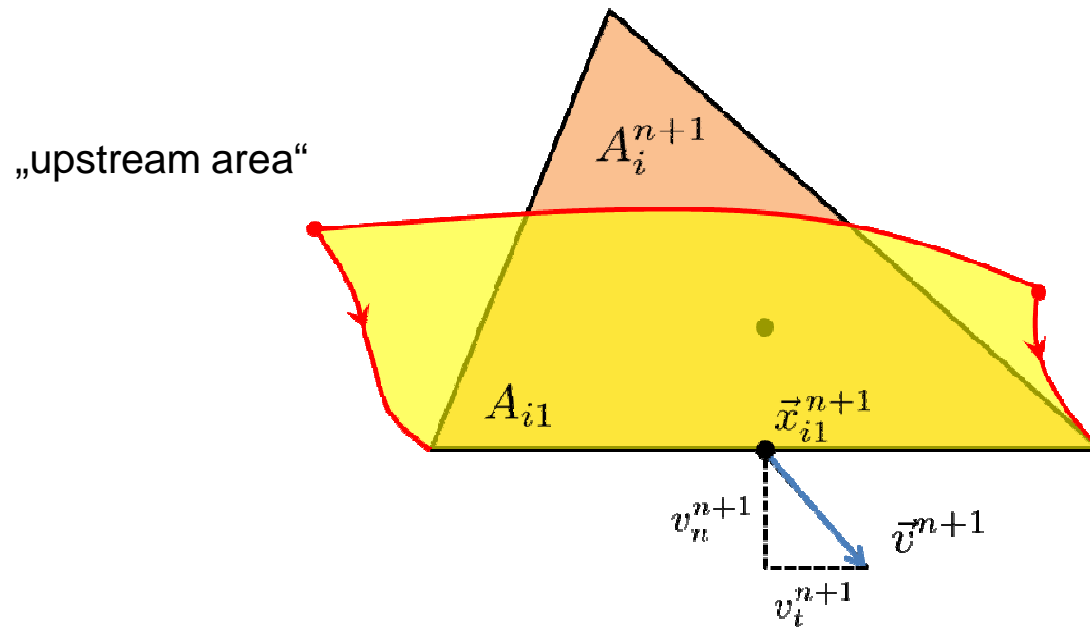


III. Currently implemented transport scheme

1. Approximation of the upstream area A_{ik}

normal component v_n^{n+1} : prognostic variable

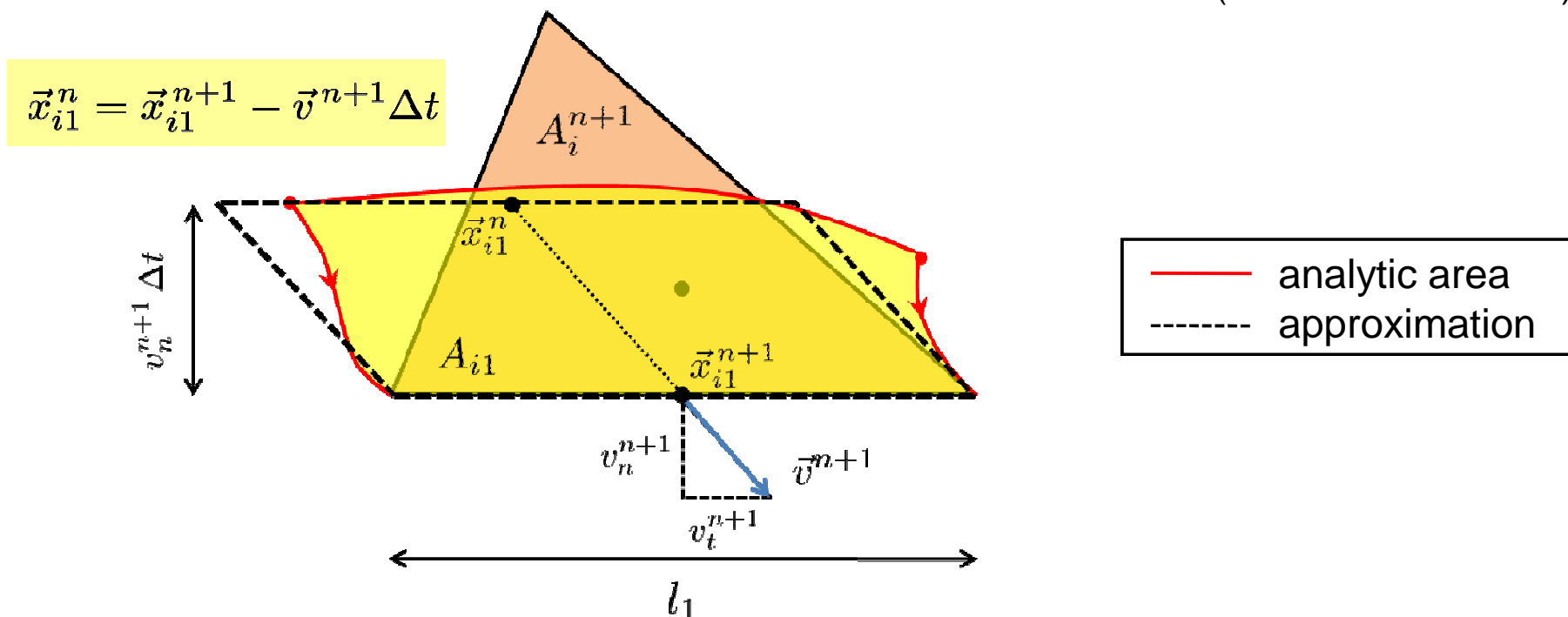
tangential component v_t^{n+1} : reconstructed via RBF
(radial basis functions)



1. Approximation of the upstream area A_{ik}

normal component v_n^{n+1} : prognostic variable

tangential component v_t^{n+1} : reconstructed via RBF
(radial basis functions)

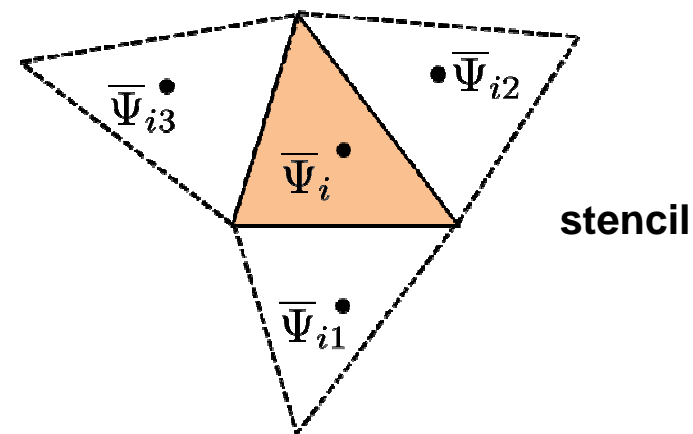


2. Approximation of subgrid distribution $\Psi(x,y,t_0)$

- Piecewise linear approximation for subgrid distribution $\Psi(x, y, t_0)$

$$\Psi^R(\vec{x} - \vec{x}_i) = \underbrace{\Psi|_{\vec{x}_i}}_{\text{unknown}} + \underbrace{\frac{\partial \Psi}{\partial x}}_{\text{unknown}} \Big|_{\vec{x}_i} (x - x_i) + \underbrace{\frac{\partial \Psi}{\partial y}}_{\text{unknown}} \Big|_{\vec{x}_i} (y - y_i) \quad (x_i, y_i) : \text{mass point of control volume } i$$

- unknowns are chosen to **conserve the mean value $\bar{\Psi}_i$ in the control volume** i and to **minimize the error** in predicting the mean values $\bar{\Psi}_{i1}, \bar{\Psi}_{i2}, \bar{\Psi}_{i3}$ for control volumes in the stencil.



- For each control volume i :

4 equations for 3 unknowns $\Psi|_{\vec{x}_i}, \frac{\partial \Psi}{\partial x} \Big|_{\vec{x}_i}, \frac{\partial \Psi}{\partial y} \Big|_{\vec{x}_i}$



weighted least squares reconstruction

3. Integrate subgrid distribution

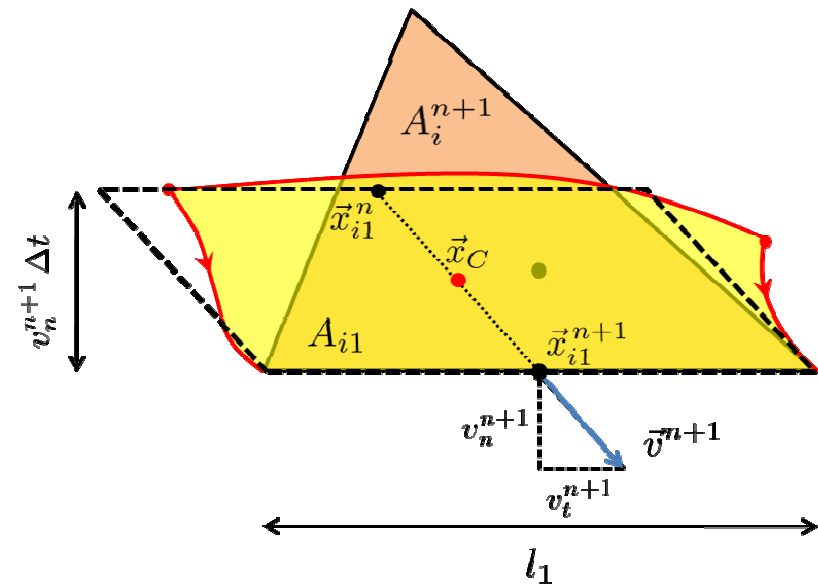
1. Upstream area A_{i1} ✓
2. Subgrid distribution $\Psi(x,y,t_0)$ ✓
3. **Integration**

$$\vec{F}_{i1} \cdot \vec{n}_{i1} = \iint_{A_{i1}} \Psi(x, y, t_0) dA = A_{i1} \bar{\Psi}_{A_{i1}}$$

upstream area: $A_{i1} = l_1 (v_n^{n+1} \Delta t)$

area average: $\bar{\Psi}_{A_{i1}} = \Psi^R(\vec{x}_C)$

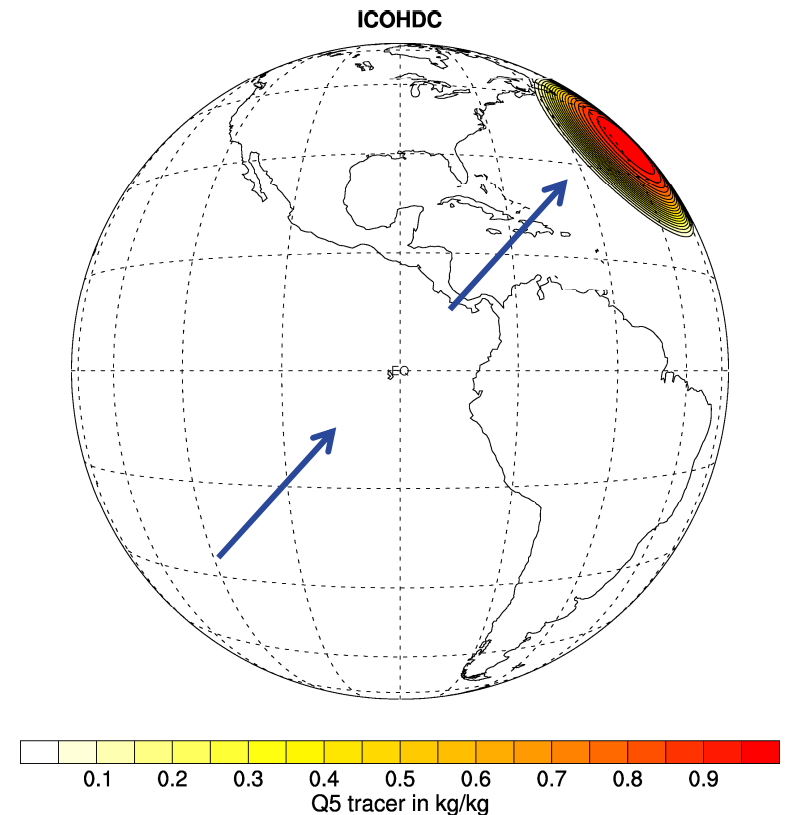
$$\vec{x}_C = \vec{x}_{i1}^{n+1} - \frac{\Delta t}{2} \vec{v}^{n+1} \quad \text{center of mass of parallelogramm}$$



IV. Results of idealised test cases on the sphere

Solid body rotation test case

- Uniform flow along northeast direction
- Initial scalar field is a cosine bell centered at the equator
- After 12 days of model integration, cosine bell reaches its initial position
- Analytic solution at every time step = initial condition

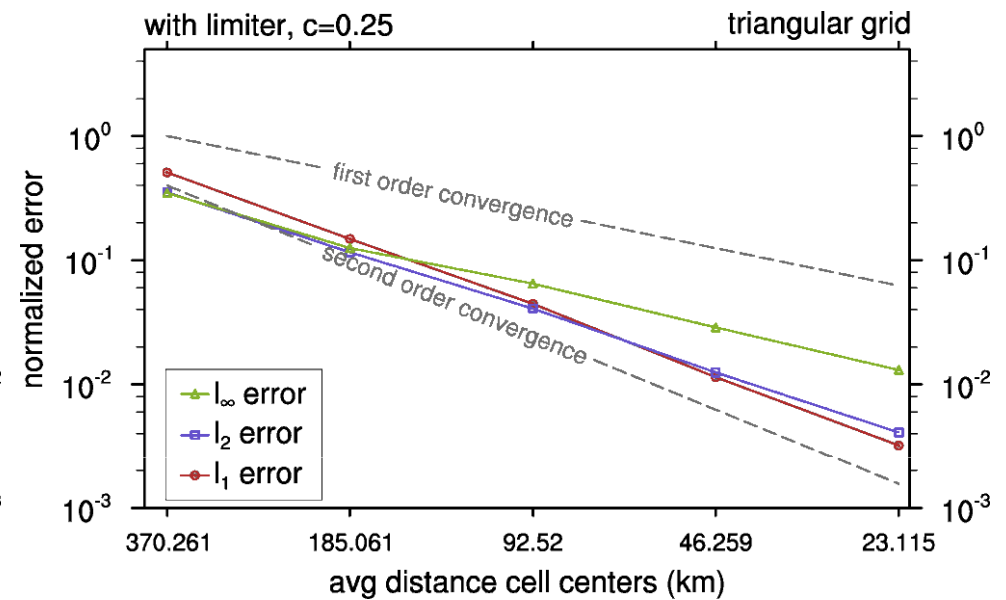
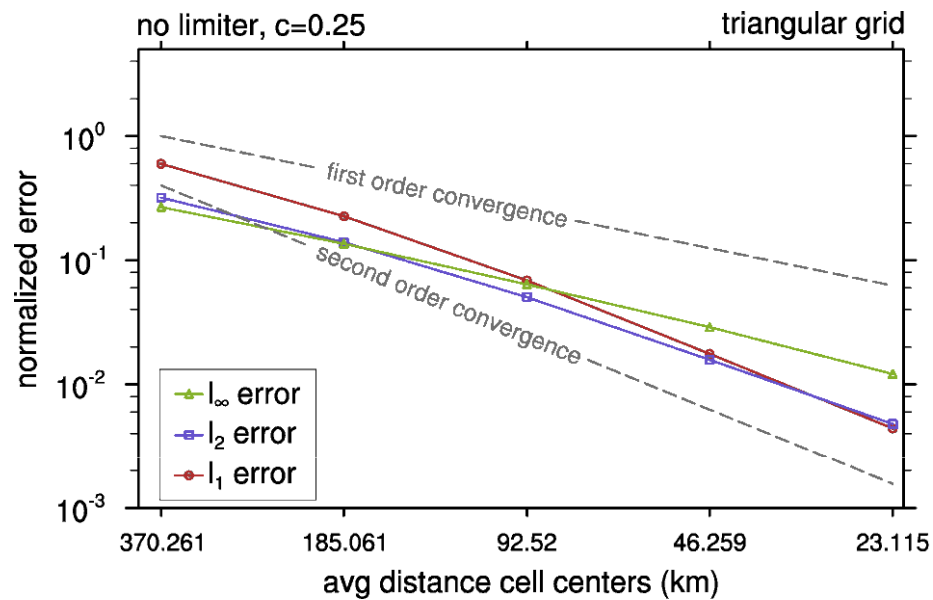


Error norms (l_1 , l_2 , l_∞) are calculated after one complete revolution for different resolutions

Error norms (solid body rotation)

$c \approx 0.25$, without limiter

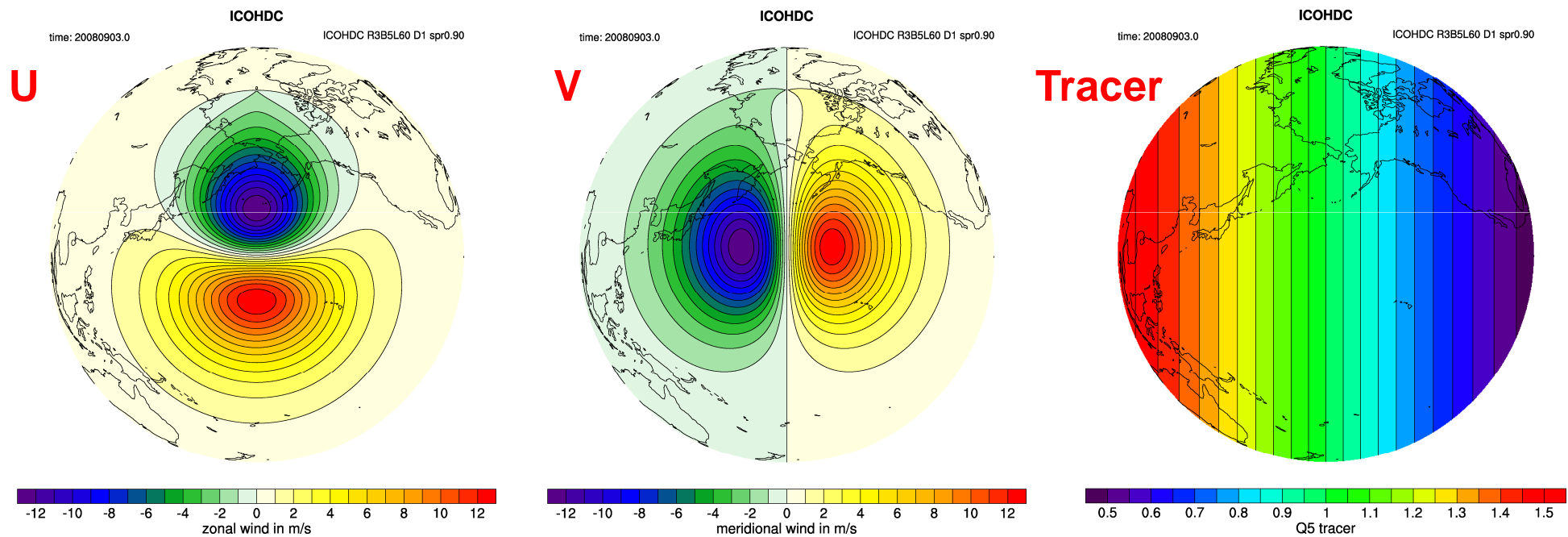
$c \approx 0.25$, with limiter



- l_1 and l_2 : almost 2nd order convergence rate
- l_∞ : only close to 1st order

Static vortex test case

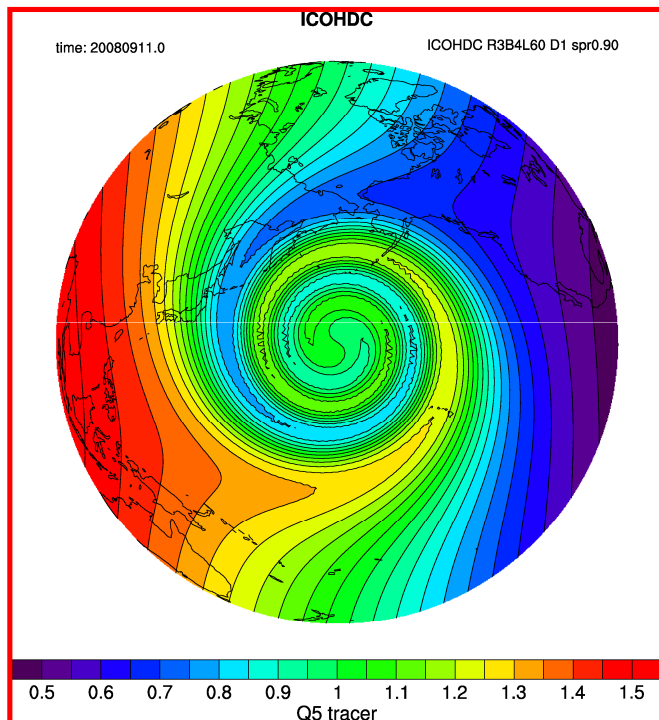
- Flow is deformational, thus more challenging than solid-body rotation
- Vortex center at $(\lambda, \varphi)=(180^\circ, 37.5^\circ)$
- U, V constant in time
- Comparison against analytical solution



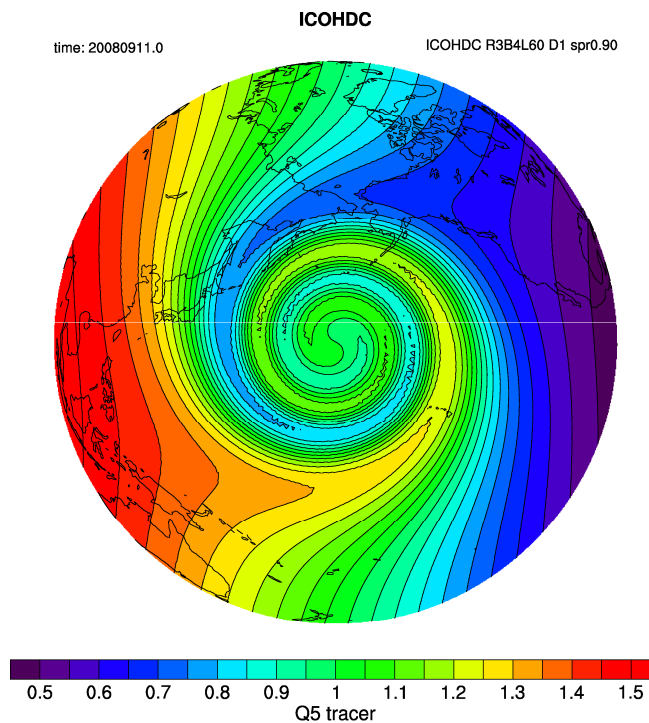
Results after 10 days

- Resolution: R3B4 (≈ 92 km)
- Courant number $c \approx 0.1$

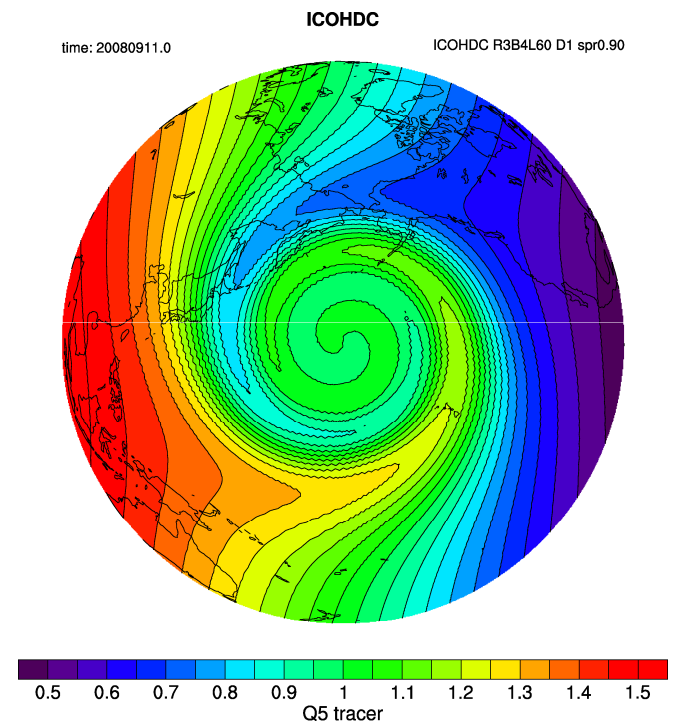
Analytic solution



our scheme (Miura)

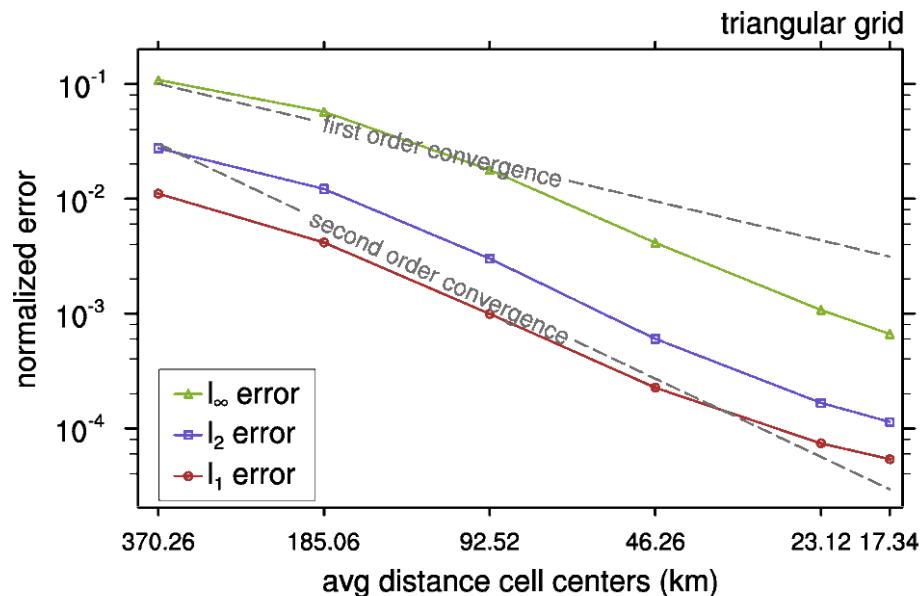


upwind

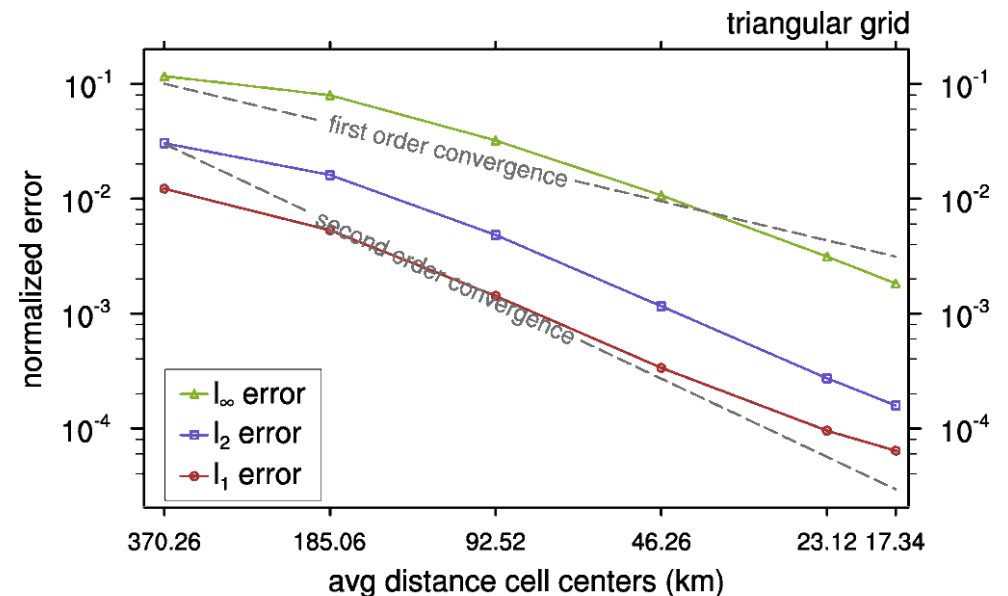


Error norms (static vortex)

$c \approx 0.25$, without limiter



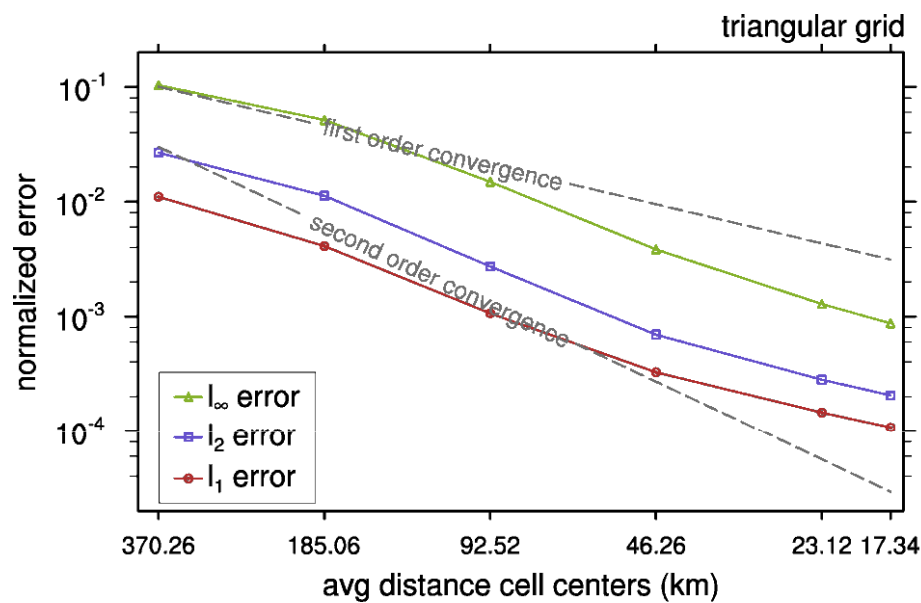
$c \approx 0.25$, with limiter



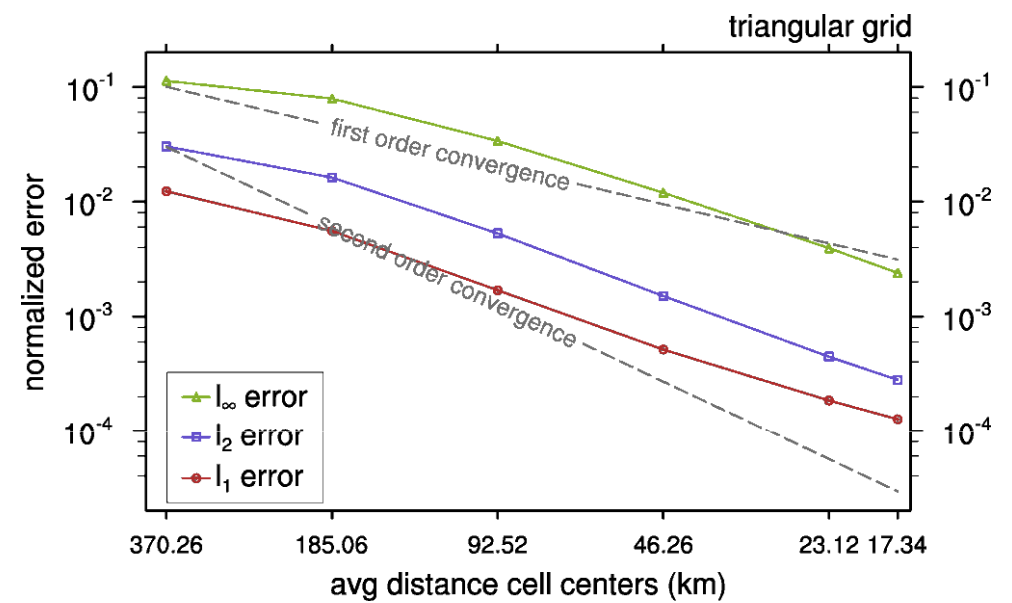
- **no limiter:** almost 2nd order convergence for medium-high resolution, but convergence rate decreases for very high resolution.
- **with limiter:** slightly increasing absolute error and slightly decreasing convergence rates

Error norms (static vortex)

$c \approx 0.6$, without limiter



$c \approx 0.6$, with limiter



V. Summary and outlook

- transport schemes in ICON are still **work in progress**
- current horizontal **advection scheme is similar to the scheme of Miura (2007)**.
- based on combined semi-Lagrangian finite-Volume thinking (subgrid streamline integration method)
- **formally second order accurate**
- observed convergence rates are **slightly worse than second order** (for $c \approx 0.25$) and slightly decrease for higher Courant numbers.

Outlook:

- More testing required
- pushing towards **third order accuracy**
 - Use quadratic instead of linear reconstruction
 - Improve approximation of the upwind area (use reconstructed velocities at vertices)
 - Involves explicit numerical integration of

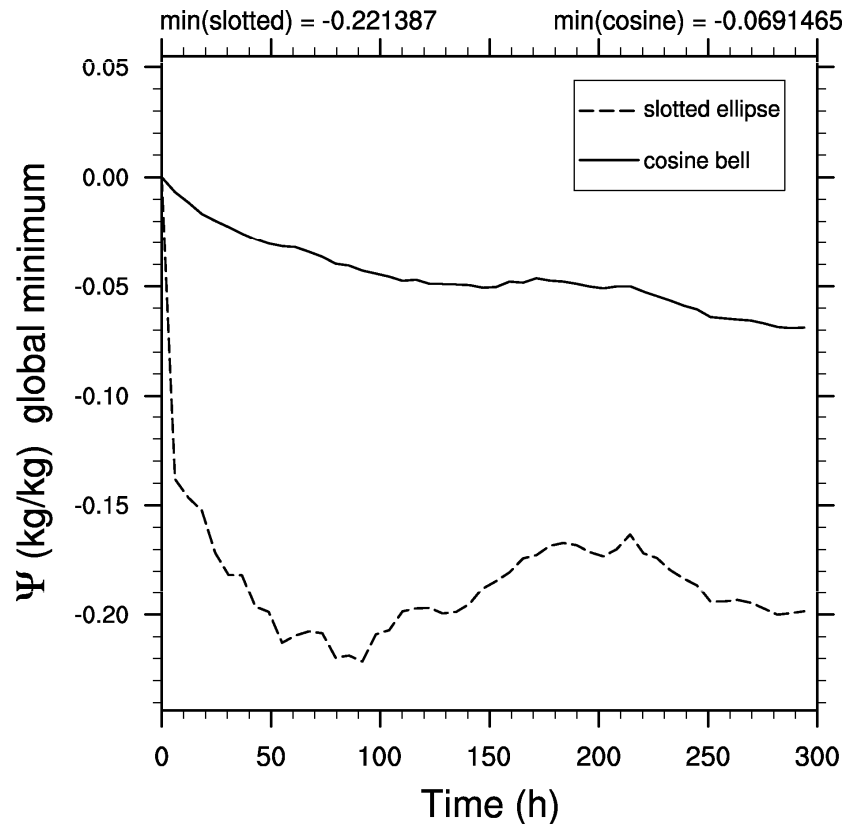
$$\iint_{A_{ik}} \Psi(x, y, t_0) dA$$



Thank you for your attention !!



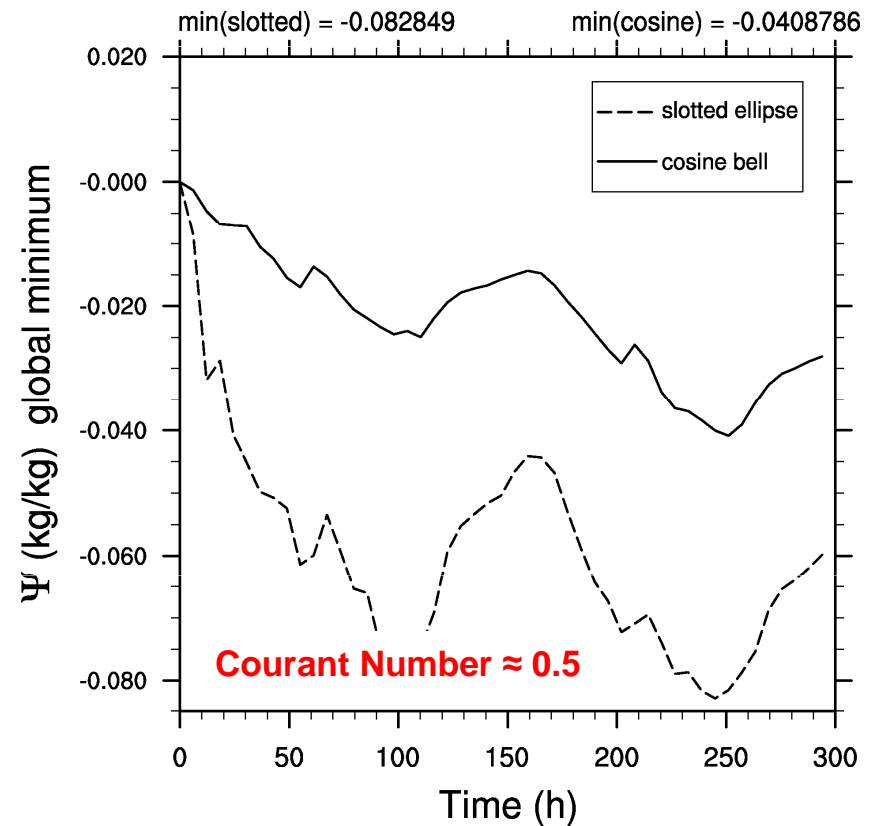
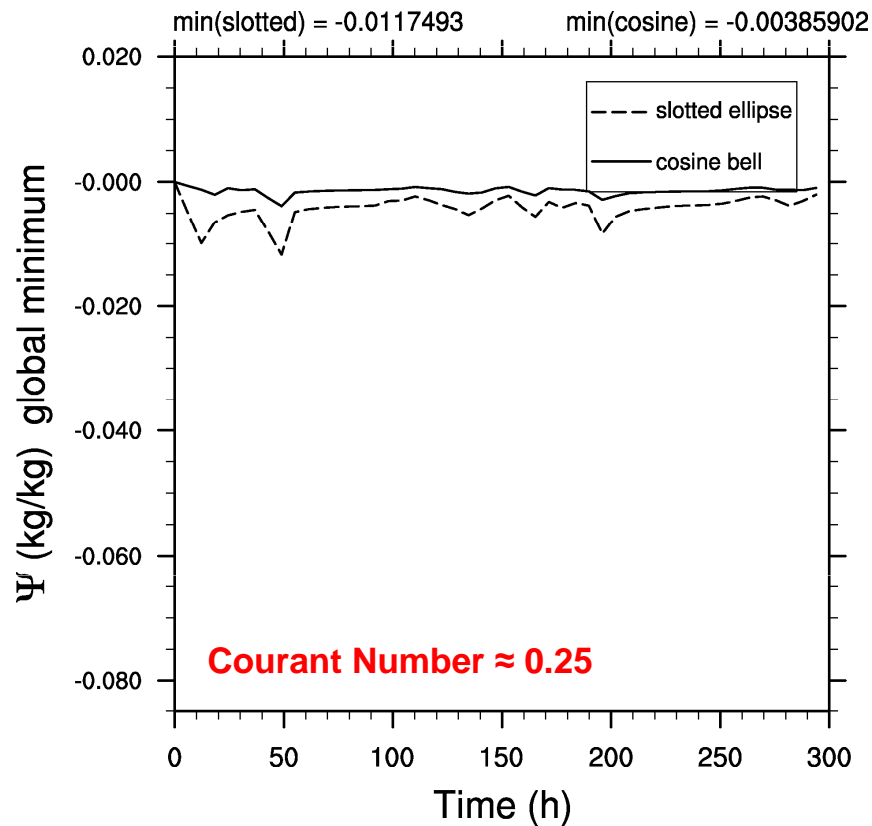
Slope limiting



➤ Initial conditions: $0 \leq \Psi \leq 1$

➤ Scheme is non-monotonous

Standard Barth-Jespersen limiter



- Not able to fully eliminate over- and undershoots

Modified Limiter

